

Rotor Asymmetries Faults Detection in Induction Machines under the Impacts of Low-Frequency Load Torque Oscillation

Mohammad Hoseintabar Marzebali, Reza Bazghandi, Vahid Abolghasemi, *Senior Member*

Abstract—Low-frequency torque oscillations (LTOs) characteristic components emerge in the stator current spectrum of induction machines (IMs) as additive frequencies near the rotor asymmetry fault (RAF) indices especially in gearbox-based electromechanical system. The interactions between these two components make the fault detection process complicated and lead to false alarm.

In this paper, a new technique for detection and separation of RAF from LTOs in IMs based on single phase stator current data is proposed. The method benefits from a novel pre-processing stage based on several sign functions. Hence, a two-axis rotating reference frame with a single phase of stator current of IMs with no prior knowledge of the rotational speed is introduced. The proposed method maps the static reference frame obtained through single stator current and its associated Hilbert transform to the proposed rotating reference frame which can separate the effects of LTOs from RAF, effectively. The validity of the proposed technique is tested through theoretical analysis, and experiments in both steady-state and transient conditions. In this regard, Synchro-squeezing Wavelet Transforms (SWT) is used for time-frequency analysis of faulty stator current in transient conditions. The obtained results confirm the effectiveness of the proposed approach to separate the RAF characteristic frequency from LTOs even in line-fed IMs applications.

Index Terms—Condition monitoring, fault diagnosis, fast Fourier transform, stator current analysis, induction machine.

NOMENCLATURE

T_l	Load torque.
T_{em}	Electromechanical torque.
T_{osc}	Torque oscillation component.
f_{LTO}	Load torque oscillation frequency.
I_s	Stator current amplitude.
I_r	Rotor current amplitude.
β	Modulation index of LTOs.
φ	Phase difference.
f_s	Supply frequency.
f_r	Rotor frequency.

p
 s
 J_n
 G
 γ
 f_{RAF}

Pole pairs.
 Slip.
 n^{th} order of Bessel function.
 Ratio of speed reduction.
 Modulation index of RAF.
 Characteristic frequency of RAF.

I. INTRODUCTION

INDUCTION machines have been extensively used in different industrial applications such as traction systems, and wind turbines due to remarkable advantages over other types of electrical machines [1,2]. Condition monitoring of IMs are necessary and inevitable due to IMs working in harsh environmental conditions or sensitive applications [3].

IMs are normally faced with different electrical and mechanical failures including rotor asymmetry faults (RAF), dynamic and static eccentricity, and inter-turn faults [4]. A significant failure rate in IMs is related to RAF which occurs in the wound rotor induction machines (WRIMs) and squirrel cage induction machines (SCIMs) as unbalance rotor winding and broken rotor bars, respectively [5,6]. In this regard, different methods for condition monitoring of electrical machines have been presented in recent years. Among them, motor current signature analysis (MCSA) due to simplicity and non-invasive nature has been attracted more attention [7, 8]. Up to now, countless pre-processing techniques have been presented to detect and demodulate mechanical and electrical faults from main supply frequency in the stator current spectrum of IMs. Some of the well-established ones are Teaser-Kaiser [9], rectified stator current [5], and analytic signal based on Hilbert transform [10].

One of the major problems in the process of RAF detection in the spectrum of stator current is related to the interaction between low torque oscillations (LTOs) and RAF indices which leads to false alarm [11]. The existing methods for separating the characteristic of RAF from LTOs can be divided into non-invasive and invasive techniques. In non-invasive methods, there is no need to install and use additional sensors to record data of signals. Invasive methods, such as flux-based methods, would require the installation of external sensors in the form of coils or an air-gap flux sensors in the stator slots.

Mohammad Hoseintabar Marzebali, and Reza Bazghandi are with the school of Electrical Engineering, Shahrood University of Technology, Shahrood, Iran,

Vahid Abolghasemi is with the School of Computer Science & Electronic Engineering, University of ESSEX, Colchester Campus, UK.

(Corresponding author: Mohammad Hoseintabar Marzebali, m.hoseintabar@shahroodut.ac.ir).

Table I: summary of the comparison of the methods presented in recent years

Method	Signal	Number of sensors	RAFs index	LTOs index	Transient analysis	Demodulation	Comments
Rectified Stator Current Signature [5]	Current	1	$2sf_s$	f_{LTO}	×	✓	<ul style="list-style-type: none"> The method is simple and can be easily implemented The method cannot be able to isolate and separate LTOs from RAF indices
Square of Stator Current [5]	Current	1	$2sf_s$	f_{LTO}	×	✓	<ul style="list-style-type: none"> The method cannot be able to isolate and separate LTOs from RAF indices The amplitudes of RAF and LTOs indices due to multiplication process are changed.
Space Harmonics [11]	Current	1	$(5 \times (1-s) \pm s)f_s$	×	✓	×	<ul style="list-style-type: none"> The method was tested on startup current for transient analysis to observe RAFs characteristic frequency in low frequency wavelets (Not acceleration or deceleration conditions). The high frequency harmonics of machines are severely attenuated due to inherent transfer function of machine [4].
Positive and Negative Sequences of Stator Current [12]	Current	3	$2sf_s$	f_{LTO}	×	✓	<ul style="list-style-type: none"> The method cannot be applicable for IM in the closed-loop application with speed controller. Inherent asymmetry in motor and supply voltage makes this method complicated in the line-fed IMs applications. The speed of IMs for calculation of currents in rotating reference frame need to be known.
Instantaneous Active and Reactive Currents [15]	Current/Voltage	6	$(1 \pm 2s)f_s$	$f_s \pm f_{LTO}$	×	×	<ul style="list-style-type: none"> The high number of sensors make the implementation of this method complicated.
Flux-based fault detection [17,29]	Flux	1	$\frac{2sf_s}{(1 \pm 2s)f_s \pm f_r}$	$f_s \pm f_{LTO}$	×	-	<ul style="list-style-type: none"> External flux sensor need to be installed. Flux-based sensor is sensitive to the place of installation.
Mechanical rotor speed [30]	Speed	1	$2sf_s$	f_{LTO}	✓	-	<ul style="list-style-type: none"> Invasive method Mechanical speed sensor need to be installed. The method is tested in startup condition. Inability to separate and isolate between RAFs and LTOs.
Air-gap flux based detection [31]	Flux	1	$(1 \pm 2s)f_s$	$f_s \pm f_{LTO}$	✓	-	<ul style="list-style-type: none"> Need to be installed in the stator tooth surface Invasive method Inability to separate and isolate between RAFs and LTOs. The method is tested in startup condition. Since the slip change due to testing system in startup condition from 0 to 1, it can be deduced that the method is independent of load.
Fundamental Frequency Normalization Technique [32]	Current	1	$(1 \pm 2s)f_s$	$f_s \pm f_{LTO}$	✓	✓	<ul style="list-style-type: none"> Inability to separate and isolate between RAFs and LTOs. The method is tested in startup condition. The mechanical load anomalies generated by brake system by a sinusoid signal reference with the frequency of 4 Hz.
Proposed Method	Current	1	$2sf_s$	f_{LTO}	✓	✓	<ul style="list-style-type: none"> The method cannot be applicable for IM in the closed-loop application with speed controller

Since the non-invasive methods are simple, cost-effective and do not require additional sensors, they have received more attention. Among the methods presented in the literatures, the current-based methods are preferred to other methods. The next limiting factor is the number of sensors required for condition monitoring process in the machine. Some methods require a large number of sensors to analyze the data such as those based on three-phase condition monitoring. Moreover, demodulation of the fault signal from the supply frequency helps to prevent the leakage of the main frequency. Some papers make the detection RAF in the presence of LTOs based on the use of machine start-up current signal. However, these methods can only be used for analyzing the machine in start-up mode, which will be difficult to be implemented for many machines that are constantly working.

Elimination of broken rotor bars false indication in SCIMs based on a set of two rotating components of line currents has been introduced in [12]. To do this, positive and negative sequences of stator current were inspected. It has been shown that the modulated signal due to LTOs and RAF can be demodulated from fundamental frequency to avoid leakage effects of fundamental frequency. Moreover, LTOs and RAF can be observed and detected in two axes of rotating reference frame built by two phases of stator current, separately. Although, this method is effective in the case of machines with closed loop drive systems, inherent asymmetry in motor and supply voltage makes this method complicated in the line-fed IMs. Some model-based techniques have been used for the prevention of interaction between LTOs and RAF [13, 14]. However, knowing and estimating the detailed parameters of IMs make the use of these techniques complicated. Angular

displacement of active and reactive current space vector spectrums has been proposed for extracting RAF indices in the presence of external rotor faults [15]. The latter method needs three-phase current and voltage data for this purpose, which is a limiting factor. The main challenge of flux-based induction machines faults monitoring, which makes these flux-based methods complicated, is related to the implementation of flux sensors [16, 17]. Recently, artificial intelligence methods along with proper pre-processing step were introduced to overcome some drawbacks of pervious methods to avoid positive and negative false alarm [18, 19]. A summary of the comparison of the methods presented in recent years in this field is given in the Table I.

In summary, major load challenges in the separation of RAF indices and LTOs to avoid interaction effects between two indices and false alarm can be classified as follow:

- The effects of fundamental frequency leakage on RAF indices need to be investigated. It is necessary to note that the fundamental frequency leakage can bury the main indices of RAF in low slips.
- The method needs to be applicable in both line-fed and closed-loop applications. Some of the pervious methods require data about the machine parameters and supply voltage, which may be available in closed-loop application. However, inherent asymmetries in motor and supply voltage makes the used of these methods complicated in line-fed IMs applications.
- Number of required phases is another great limitation.

In this paper, a new technique for detection and separation of RAF from LTOs based on a single-phase signal is introduced. This signal is used for making two-axis rotating reference frame

based on sign functions to separate and demodulate fault indices from LTOs and fundamental frequency. Therefore, the main contributions of this research are as follows:

- A new method based on a single-phase data is presented to create a two-axis rotating reference frame for line-fed induction machine without measuring the speed of machine.
- Extensive experiments are conducted to demonstrate the effectiveness of using the proposed method to demodulate RAF indices from main frequency.

II. PROBLEM DESCRIPTION

In this section, mathematical description of characteristic frequencies related to LTOs and RAF in IMs are provided. Furthermore, the interactions between these two characteristic frequencies in the spectrum of stator current are evaluated. In this regard, stator current signal in the presence of LTOs and RAF is modeled both analytically and by means of modeled stator current signal.

A. LTOs effects on the stator current signature of IMs

LTOs occur due to load fluctuations, imperfect connection between different mechanical components of drive-train and defect on the structure of electromechanical systems. LTOs lead to fluctuations proportional to rotational frequency in the torque of machine (1) [20].

$$T_l = T_{em} + T_{osc} \sin(2\pi f_{LTO} t), \quad (1)$$

It has been shown by analytical and experimental evaluations that torque oscillations lead to phase modulation of rotor current. The simplified description of stator current (i_{s_LTO}) can be written as follows:

$$i_{s_LTO}(t) = I_s \cos(2\pi f_s t + \varphi) + I_r \cos(2\pi f_s t + \beta \sin(2\pi f_{LTO} t)), \quad (2)$$

Expansion of (2) through Bessel series shows that sidebands frequencies of LTOs (f_{LTO}) emerges around the supply frequency (3), (4).

$$i_{s_LTO}(t) = I_s \cos(2\pi(f_s)t + \varphi) + I_r \sum_{n=-\infty}^{n=\infty} J_n(\beta) \cos(2\pi(f_s + n f_{LTO})t + \varphi), \quad (3)$$

$$f_{LTO} = f_s \pm k f_{LTO} = f_s \pm k(1-s)f_s / Gp; \quad k = 1, 2, 3, \dots \quad (4)$$

With considering the main harmonics of i_{s_LTO} ($n=1$), (3) can be simplified as (5) [21].

$$i_{s_LTO}(t) = I_s \cos(2\pi f_s t + \varphi) + I_s J_1(\beta) \cos(2\pi(f_s + f_{LTO})t) + I_s J_{-1}(\beta) \cos(2\pi(f_s - f_{LTO})t), \quad (5)$$

LTOs effects can be detected as sideband frequencies around the main frequency as it can be observed in (5).

B. RAFs effects on the stator current signature of IMs

Some faults gradually increase from its incipient stage to severe conditions. One of these faults is RAF, which appears as broken bars in squirrel cage induction machines (SCIM), or high resistance connections (HRC) in WRIM [22-24]. Generally, HRC occurs due to variation in amplitude of resistance of phases of machine or short circuit in the windings of rotors, which leads to asymmetry in the rotor windings. RAF causes local heating and consequently serious damage to the structure and operation of IMs. RAF generates amplitude modulation in the stator current of IMs with following characteristics.

$$f_{RAF} = (2\zeta s)f_s; \quad \zeta = 1, 2, 3, \dots \quad (6)$$

The simplified analytical description of stator current in the presence of RAF can be written as (7).

$$i_{s_RAF}(t) = I_s \cos(2\pi f_s t) (1 + \gamma \cos(2\pi f_{RAF} t)), \quad (7)$$

With considering, the first main harmonics of RAF, (7) can be simplified as:

$$i_{s_RAF}(t) = I_s \cos(2\pi f_s t) + \frac{\gamma}{2} I_s \cos(2\pi f_s (1-2s)t) + \frac{\gamma}{2} I_s \cos(2\pi f_s (1+2s)t), \quad (8)$$

It can be deduced from (8) that rotor asymmetries effects can be observed as additive sideband frequencies around the supply frequency (f_s).

C. Interaction between characteristic frequencies of RAF and LTOs on stator current signature

RAF and LTOs generate specific characteristic in the spectrum of stator current of IMs. LTOs may cause false alarm in case of gearbox-based electromechanical system. In fact, the interaction between these characteristics makes fault detection process complicated. The characteristic frequency of LTOs due to the presence of speed reduction couplings approaches to the RAF, which leads to false alarm. This issue is related to the values of G and p (4). Increase in the values of G and p causes LTOs characteristic frequency to get closer to the RAF characteristic frequency. Therefore, proper detection techniques, which can separate these two fault characteristic indices, need to be used. The simplified analytical model of stator current in the presence of RAF and LTOs (i_{s_a}) with considering (2) and (8) can be written as [12]:

$$i_{s_a}(t) = I_s \cos(2\pi f_s t) + \frac{\gamma}{2} I_s \cos(2\pi f_s (1-2s)t) + \frac{\gamma}{2} I_s \cos(2\pi f_s (1+2s)t) + I_r \cos(\omega_s t + \beta \sin(2\pi f_{LTO} t)), \quad (9)$$

Equation 9 is a simple description of RAF as well as the LTOs of the machine, each of which is described separately in the previous sections. In reality, these equations would become much more complicated due to the modulation and the dynamic

behavior of the machine. This simplified model has been considered to investigate the amplitude and phase modulations of such effects. It is worth mentioning that these equations are inspired by the equations presented in [12].

III. PROPOSED METHOD: ANALYTICAL APPROACH

Previously, two main approaches have been presented for separation of RAF and LTOs fault indices in stator current signature. In this regard, space harmonics generated by the non-sinusoidal distribution of stator windings was considered for single-phase stator current signature analysis. However, weakness of space harmonics makes the detection and the separation complicated. In the second approach, monitoring of positive and negative sequence information of three-phase stator current signature in closed loop drive are proposed which cannot be applicable for line-fed IMs [11,12].

As it has been explained in section II, amplitude and phase modulation of stator current occurs due to RAF and LTOs, respectively. The goal of the proposed method is to separate those effects to avoid interaction between fault characteristic frequencies. Therefore, three objectives are considered here: 1) single-phase current data analysis 2) demodulation of fault characteristic frequencies from supply frequency, and 3) separation of RAF and LTOs fault indices.

A. Two-axis stationary reference frame with one phase current based on Hilbert transform ($\alpha\beta$)

The stationary reference frame components with three phases of stator currents have two stationary axes, which include the specification of faults and 90° phase differences. However, three-phase stator current of IMs need to be transformed through Clark transformation to construct two-axis stationary reference frame. Consequently, the cost of condition monitoring system with three-phase current sensor increases. As solution, a two-axis rotational reference frame with only single-phase stator current of IMs based on Hilbert transform is used for this purpose, which is explained as follow:

The Hilbert transform ($H(x(t))$) of real time signal ($x(t)$) is defined as follow:

$$H(x(t)) = \tilde{x}(t) = \frac{1}{\pi} \int_{-\infty}^{+\infty} \frac{x(\tau)}{t - \tau} d\tau, \quad (10)$$

With considering the mean value Theorem, the Hilbert transform of ($H(x(t))$) is obtaining by calculating the convolution between function of $1/\pi t$ and the original signal ($x(t)$) which can be rewritten as (10) [25].

$$\tilde{x}(t) = \frac{1}{\pi t} * x(t), \quad (11)$$

The Fourier transform of ($H(x(t))$) is

$$H(f) = X(f)[-j \operatorname{sgn}(f)], \quad (12)$$

where

$$\operatorname{sgn}(x) = \begin{cases} -1 & x < 0 \\ 0 & x = 0 \\ 1 & x > 0 \end{cases} \quad (13)$$

It means that the positive and negative frequencies of the spectrum of $x(t)$ are shifted by -90° and $+90^\circ$ by Hilbert transform, respectively. In other words, the Hilbert transform

can be considered as a filter with the amplitude of unit and $\pm 90^\circ$ phase differences, which depends on the sign of the frequency of the original signal.

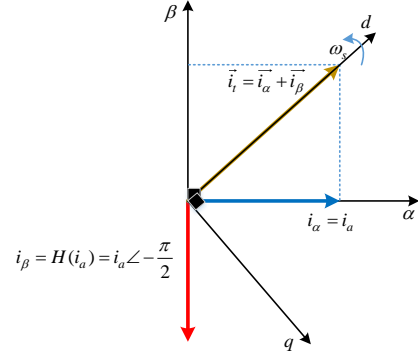


Fig.1. Stationary reference frame

In this paper, considering Hilbert transform, single-phase stator current is defined in $\alpha\beta$ stationary reference frame as (see Fig.1 for visual inspection):

$$\begin{cases} i_\alpha = i_a(t), \\ i_\beta = H(i_a(t)), \end{cases} \quad (14)$$

The simplified analytical model of the stator current by considering (14) can be expressed as:

$$\begin{cases} i_\alpha(t) = I_s \cos(2\pi f_s t) + \\ \quad + \frac{\gamma}{2} I_s \cos(2\pi f_s (1-2s)t) + \\ \quad + \frac{\gamma}{2} I_s \cos(2\pi f_s (1+2s)t) + \\ \quad + I_r \cos(\omega_s t + \beta \sin(2\pi f_{LTO} t)), \\ i_\beta(t) = I_s \cos(2\pi f_s t - \frac{\pi}{2}) + \\ \quad + \frac{\gamma}{2} I_s \cos(2\pi f_s (1-2s)t - \frac{\pi}{2}) + \\ \quad + \frac{\gamma}{2} I_s \cos(2\pi f_s (1+2s)t - \frac{\pi}{2}) + \\ \quad + I_r \cos(\omega_s t + \beta \sin(2\pi f_{LTO} t) - \frac{\pi}{2}), \end{cases} \quad (15)$$

B. The proposed rotating reference frame (dq)

In order to separate the fault characteristics frequencies related to the RAF and LTOs, a new mapping from $\alpha\beta$ static reference frame to direct and quadrature orthogonal rotating reference frame named dq is introduced. It is necessary to note that the proposed rotating reference frame also can be used for line-fed applications of IMs and does not need any information regarding the rotational speed of IMs which is the main drawback of some pervious methods presented in the literature.

$$\begin{bmatrix} i_d \\ i_q \end{bmatrix} = \begin{bmatrix} \operatorname{sgn}(i_\alpha) & \operatorname{sgn}(i_\beta) \\ \operatorname{sgn}(i_\beta) & -\operatorname{sgn}(i_\alpha) \end{bmatrix} \begin{bmatrix} i_\alpha \\ i_\beta \end{bmatrix} \quad (16)$$

where $i_\alpha \times \operatorname{sgn}(i_\alpha)$ and $i_\beta \times \operatorname{sgn}(i_\beta)$ are the rectified currents of stator in the axes of α and β . The expression of $\operatorname{sgn}(i_\alpha)$ and $\operatorname{sgn}(i_\beta)$ are in the forms of square waves and can be simply described based on dominant frequency of stator current (f_1) as

$\text{sgn}(\cos(2\pi f_1 t))$ and $\text{sgn}(\sin(2\pi f_1 t))$, respectively. The expansion of $\text{sgn}(\cos(2\pi f_1 t))$ and $\text{sgn}(\sin(2\pi f_1 t))$ as series can be written as (14) and (15).

$$\text{sgn}(\cos(2\pi f_s t)) = \frac{4}{\pi} \sum_{n=1,3,5,\dots}^{\infty} \left[\frac{\sin(\frac{n\pi}{2})}{n} \cos(2\pi f_s t) \right], \quad (17)$$

$$\text{sgn}(\sin(2\pi f_s t)) = \frac{2}{\pi} \sum_{n=1,3,5,\dots}^{\infty} \left[\frac{2\cos(\frac{n\pi}{2}) - \cos(n\pi) - 1}{n} \cos(2\pi f_s t) \right], \quad (18)$$

Considering the first harmonics of (17) and (18), transformation matrix can be rewritten as:

$$\begin{bmatrix} i_d \\ i_q \end{bmatrix} = \frac{4}{\pi} \begin{bmatrix} \cos(2\pi f_s t) & \sin(2\pi f_s t) \\ \sin(2\pi f_s t) & -\cos(2\pi f_s t) \end{bmatrix} \begin{bmatrix} i_\alpha \\ i_\beta \end{bmatrix} \quad (19)$$

The transformation of stator current signature from $\alpha\beta$ into the synchronous coordinate's dq allows separating RAF and LTOs. In this regard, the d -axis of rotating reference frame demodulates the RAF from supply frequency.

$$\begin{cases} i_d = I_s + \gamma I_s \cos((2sf_s)t) + I_r \cos(\beta \sin(2\pi f_{LTO}t)) \\ i_q = -I_r \sin(\beta \sin(2\pi f_{LTO}t)) \end{cases}, \quad (20)$$

Since, amplitude of $\beta \ll 1$ and $|\sin(2\pi f_{LTO}t)| \leq 1$, (20) can be simplified as

$$\begin{cases} i_d \approx I_s + I_r + \gamma I_s \cos((2sf_s)t) \\ i_q \approx -I_r \beta \sin(2\pi f_{LTO}t) \end{cases}, \quad (21)$$

It can be deduced from (20) that the spectrum of i_d and i_q have fault characteristics of RAF and LTOs, respectively. Therefore, the interaction between RAF and LTOs can be effectively separated to avoid false alarm. The flowchart of the proposed method is illustrated in Fig. 2.

The letters d and q are direct and quadrature orthogonal rotating reference frame, respectively. By means of rotating d and q axes with the rotational frequency of the dominate frequency of the signal, the stationary two-axis reference frame can transfer the main harmonic to the zero frequency. In fact, the two-axis rotating reference frame in three-phase systems is used to transform the time-variation voltage and current variables to the constant values so that it can be used in control systems and modeling of electrical machines. In this paper, a stationary orthogonal two-axis reference frame transformation named $\alpha\beta$ is used to map a single phase of a machine on two axes using a Hilbert transform. The purpose of this work is to produce two signals that have a phase difference of 90 degrees with each other. Then, by means of proposed sign-based matrix, the stationary reference frame is transformed to the proposed dq axes, which is used for fault detection process. In this regard, the method does not need any information about the speed of machine because of sign-based function and can demodulate the fault characteristic frequency from supply frequency in order to avoid leakage effects of the main frequency.

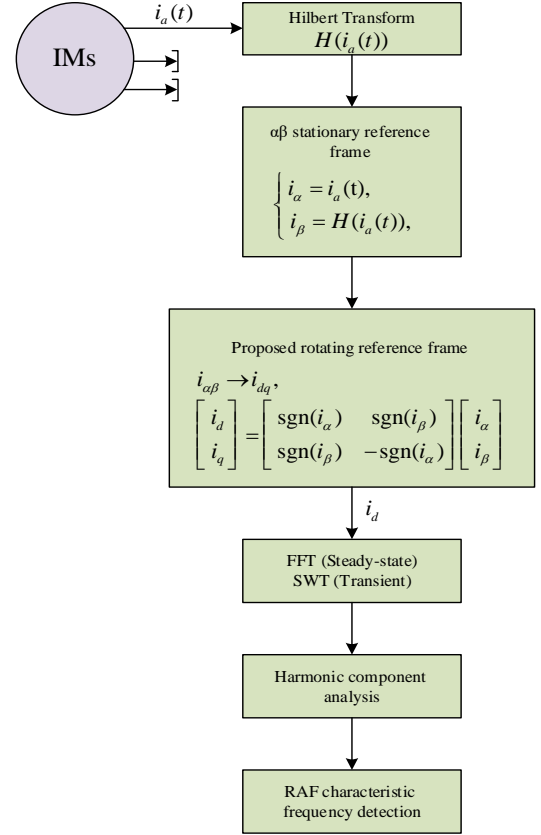


Fig. 2. Flow chart of proposed method.

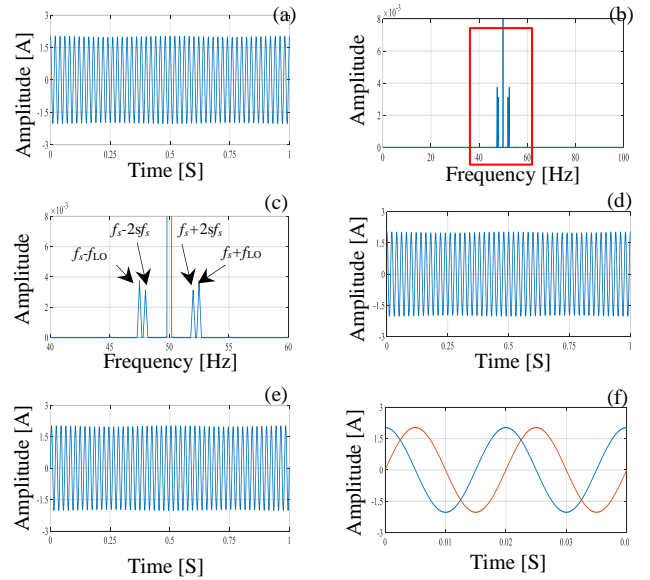


Fig. 3. Spectral analysis of proposed method using synthetic faulty stator current with sampling frequency of 10kHz and $f_s=50$ Hz, $s=0.02$, $f_{LTO}=2.5$ Hz, $I_s=1$, $I_r=1$, $\gamma=0.05$ and $\beta=0.03$ -a) $i_\alpha(t)$ -b) $i_\alpha(f)$ [0Hz-100Hz] -c) $i_\beta(f)$ [40Hz-60Hz] -d) $i_\alpha(t)$ -e) $i_\beta(t)$ -f) phase difference between $i_\alpha(t)$ and $i_\beta(t)$.

IV. PERFORMANCE EVALUATION (SYNTHETIC SIGNALS)

To ensure the accuracy of the proposed method, an evaluation procedure using synthetic data is conducted. For this purpose, a signal with mathematical expression in (8), which

has a dominant frequency $f_s=50$ Hz with the variables $s=0.02$, $f_{LTO}=2.5$ Hz, $I_s=1$, $I_r=1$, $\gamma=0.05$ and $\beta=0.03$ is considered (Fig.3a). As shown in Fig.3b and Fig.3c, the synthetic signal has two pairs of sideband frequencies, which are caused by RAF and LTOs, around the dominant frequency (f_s).

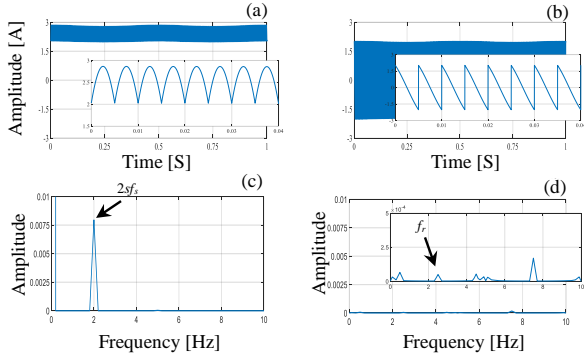


Fig.4. Spectral analysis of proposed method using synthetic faulty stator current with sampling frequency of 10kHz and $f_s=50$ Hz, $s=0.02$, $f_{LTO}=2.5$ Hz, $I_s=1$, $I_r=1$, $\gamma=0.05$ and $\beta=0.03$ -a) $i_d(t)$ -b) $i_q(t)$ -c) $i_d(f)$ -d) $i_q(f)$.

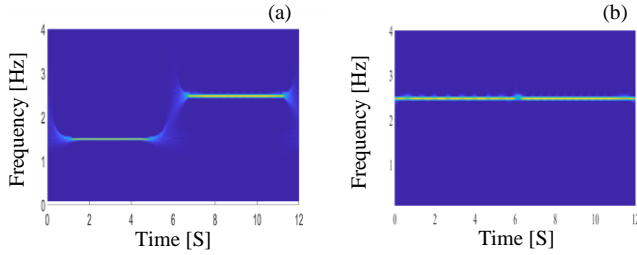


Fig.5. Time-frequency analysis of synthetic signal based on proposed method in transient condition with sampling frequency of 5kHz, $f_s=50$ Hz, $s=0.015$ (before sixth second) and $s=0.025$ (after sixth second), $f_{LTO}=2.3$ Hz (before sixth second) and $f_{LTO}=2.5$ Hz (after sixth second), $I_s=1$, $I_r=1$, $\gamma=0.05$ and $\beta=0.03$ -a) SWT of $i_d(t)$ -b) SWT of $i_q(t)$.

These two pairs of sidebands are very close to each other, so it is possible to occur false alarm (Fig.3c). For separating these two indices using the proposed method in this paper, the currents of α and β axes of the static reference frame are calculated and given in Fig.3d and Fig.3e. To understand that these two axes have a phase difference of 90 degrees due to the inherent nature of the Hilbert function, a shorter range of these two signals is plotted simultaneously in Fig.3f. Then, by means of the rotating reference frame presented in this paper, the two signals of the d and q axes are calculated and drawn in the Fig.4a and Fig.4b, respectively. Finally, the current spectra of both axes are calculated and given in Fig.4c and Fig.4d. The results show the effectiveness of the proposed method so that the characteristic frequency of RAF in the d -axis current is revealed while the LTOs effects are eliminated. Unlike i_d , the LTOs characteristic frequency is visible in the q -axis while the RAF indices are removed. It should be noted that the amplitude of the fault indices in the q -axis current is small, so it will be difficult to detect the indices in the q -axis in comparison with RAF index. Since the signal of q -axis has sharp points (Fig.4b), it needs a high sampling frequency to be able to show the amplitude and the place of each frequency accurately. By decreasing the sampling frequency, the accuracy of the

measurement will be drastically reduced, contrary to the current spectrum of the d -axis. However, detecting RAF in the d -axis current by eliminating the LTOs effects is the aim of our proposed method, which is well visible in Fig.4c.

In order to evaluate the performance of the proposed method in transient mode, the synthetic signal is evaluated first. For this purpose, it is assumed that the slip in the sixth second is changed slightly and the rest of the circuit parameters, including the frequency of the LTOs effects, are kept almost constant. Then, based on proposed method, the current signals of the defined axes d as well as q are extracted. Finally, using the Synchro-squeezing Wavelet Transforms (SWT), the i_d and i_q in time-frequency domain are obtained (Fig.5). The time-frequency method used in this paper has recently been considered and has the advantages of wavelet and EMD methods simultaneously [26-28]. The results show that the proposed method has the ability to detect and to isolate the RAF characteristic frequency from LTOs (Fig.5). Other time-frequency methods can also be used for the pre-processed signal using the proposed method. Since the frequency separation in the time domain using the SWT method, has proper clarity, SWT method was chosen to be used in this paper.

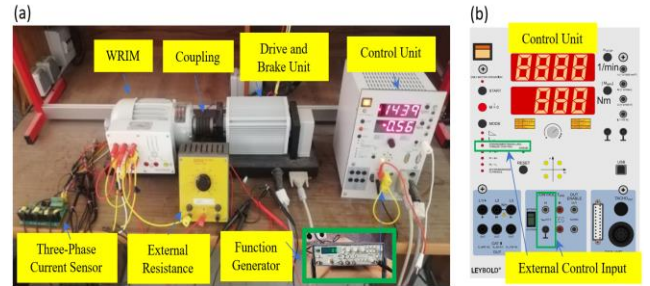


Fig.6. Test-rig system description for analysis of asymmetries in the rotor circuit of IMs -a) Test-rig -b) LTOs emulation by means of digital brake system control unit.

V. EXPERIMENTAL RESULTS

A. Test-rig description

In this section, the structure of the experimental system implemented for the evaluation of the proposed method is described. For this purpose, a 270W WRIM with available rotor terminals which have the nominal voltage of 400V, 4 poles and the rated speed of 1370 rpm is used for the fault detection process.

In order to emulate RAF, an external resistance with different values is added to the rotor circuit of the machine (R_{unb}). The measured stator current is then used for the fault detection process. Two configurations for testing the proposed method are considered in this paper. In the first configuration, a flywheel mass with inertia of 0.000612 Kgm² is linked to the motor shaft as a load. In fact, in this case, no LTOs are applied to the machine. The rotational speed of the machine due to the inherent eccentricity can be considered as LTOs in the current spectrum of machine. Due to the speed of the machine, two indices (RAF and LTOs characteristic frequencies) will be at a considerable distance from each other. The frequency of LTOs in this case does not have a significant amplitude compared to the RAFs.

In the second structure, a digital braking system is linked to the shaft of machine in which LTOs can be applied to the shaft of the studied machine in torque control mode through a function generator. In this case, LTOs, which can be observed in real systems with the presence of gearbox or deceleration couplings, can be implemented. To better mimic the overlaps between two indices, the LTO is set very close to the RAF characteristic frequency. Fig.6 shows the test-rig of the experimental system.

B. Emulation of LTOs by means of a flywheel mass

In this section, a mechanical load in form of a flywheel mass is implemented by means of a squirrel cage induction motor with the inertia of 0.000612 Kgm². The emulation of LTOs by means of flywheel mass leads to appearance of additive sidebands frequencies around the supply frequency ($f_s \pm f_r$). The stator current of a WRIM is measured under RAF. Then, according to the proposed method, a stationary reference frame with two orthogonal axes is defined, the first of which is the measured current of single stator phase, and another is the Hilbert transform of the measured phase current. It should be noted that according to the points presented in the previous sections, these two signals are 90 degrees apart in phase. Then, by means of rotating reference frame introduced in this paper, two currents, i_d and i_q , are extracted. The currents associated to the dq axes of the rotating reference frame are shown in Fig.7a and Fig.7b. The presented results are fully consistent with the simulations performed in Fig.4a and Fig.4b. The Fourier spectra of the original signal of the stator current and i_d are given in Fig.7c and Fig.7d, respectively. The spectrum of original current shows that the characteristic of the RAF is visible as sidebands around the supply frequency. These fault indices are shown in the original signal at frequencies of $(1 \pm 2s)f_s$.

The fault characteristic at $2sf_s$ frequency in the d -axis current is well visible in the Fig.7d. In this case, since the deceleration components such as the gearbox are not implemented in the drive-train of the system, the rotational frequency of the motor $f_s \pm f_r$ in the original stator current (or f_r instead of f_{LTO} in the currents of the d and q axes) is investigated. As can be seen in Fig.7e and Fig.7f, the rotational frequency of the machine, which causes false alarms, is not visible in the d -axis of current spectrum. Since the sampling frequency of the original signal is equal to 2kHz, the i_q frequency spectrum has not been evaluated. This is because the q -axis signal includes some sharp changes. Moreover, the machine used in our experiments does not have inherent eccentricity. Another important point to consider in this regard is that LTOs cause instantaneous variations in the speed of machine, which make the detection of LTOs complicated. However, the effect of the rotational frequency is visible in the q -axis current, but as the sampling frequency decreases, the accuracy of the current spectrum value will decrease. Since the objective of this paper is to detect RAFs and separate it from LTOs, the d -axis current spectrum is considered for this purpose. Therefore, with a sampling frequency of one-fifth of sampling frequency of simulation in the practical system, the fault index is still detected and the rotational frequency is eliminated.

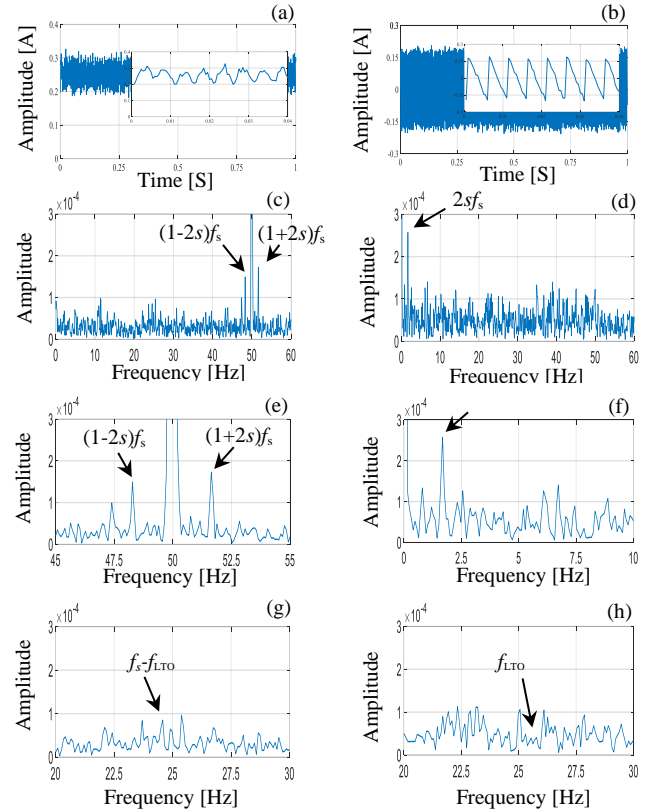


Fig.7. Experimental results in the case of emulation of LTOs by means of a flywheel mass -a) $i_d(t)$ -b) $i_q(t)$ -c) $i(f)$ [0Hz-60Hz] -d) $i_d(f)$ [0Hz-60Hz] -e) $i(f)$ [45Hz-55Hz] -f) $i_d(f)$ [0Hz-10Hz] -g) $i(f)$ [20Hz-30Hz] -h) $i_d(f)$ [20Hz-30Hz].

It is worth noting that the frequency resolution is directly proportional to the sampling frequency. It is obtained through dividing the sampling frequency by FFT size. In this study, we considered the sampling frequency of 10 kHz for the synthetic signals in both steady state and transient analysis to be able to generate Fourier spectra in different conditions with clear resolutions. This value was selected empirically so that best data representation in time and frequency is obtained. In reality, the maximum sampling frequency is limited by the capacity of the sampler and storage devices. On the contrary, the minimum sampling frequency is determined by the Shannon-Nyquist criterion. In this work, the frequencies which we are interested to detect are around 40 Hz. Hence, the sampling frequency does not need to be very high as long as it meets the Shannon-Nyquist. However, we want to have a high frequency resolution. As a result, the suitable sampling frequency we used for all our real-data experiments has been selected 2 kHz in this study.

To further validate the proposed method, real experimental data have been evaluated in acceleration (1400 to 1450 RPM) and deceleration (1450 to 1400 RPM) conditions with slightly changes in the slip of machine (Fig.8). Generally, the rotational speed variations during start-up of machines are analyzed for fault detection purpose in the literature. However, electric machines are faced to different rotational speed variations. Therefore, in this paper, the transient mode with slight rotational speed variations is investigated to confirm the resolution of the presented time-frequency method along with the validity of the proposed pre-processing method. Since the

asymmetric rotor faults can be detected from the i_d according to mathematical analysis, the d -axis current, has been evaluated and analyzed. The presented results in transient states show that the proposed method can detect and confirm the presence of RAF in the stator current of machine, appropriately (Fig.8). The variation of fault index can be tracked in the time-frequency of stator current clearly. The slip of machine varies from 0.067 to 0.032 in acceleration mode. In other words, the frequency of fault characteristic changes from 6.67 Hz to 3.33 Hz. In deceleration mode, the slip of machine based on variation in the speed of machine changes from 0.032 to 0.067. In this regard, the fault characteristic frequency varies from 3.33 Hz to 6.67 Hz.

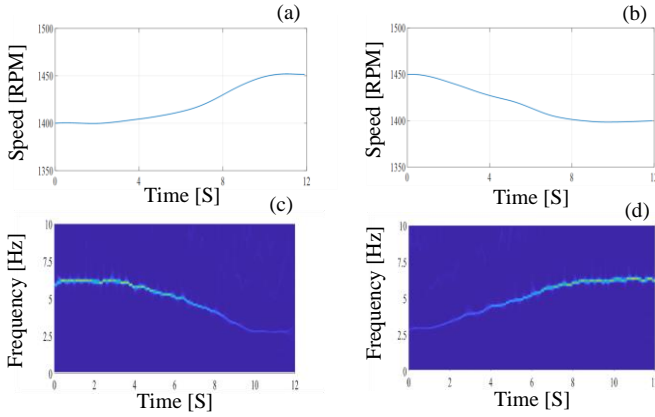


Fig.8. Time-frequency analysis of WRIG stator current with rotor asymmetry faults based on proposed method in transient condition, $f_s=50$ Hz -a) Rotational speed of WRIG in acceleration condition, -b) Rotational speed of WRIG in deceleration condition -c) SWT of $i_d(t)$ in acceleration condition -d) SWT of $i_d(t)$ in deceleration condition.

Since the characteristic frequency of RAF is directly related to the slip of the WRIM, the frequencies of $(f_s \pm f_r)$ and $(f_s \pm f_{RAF})$ are not sufficiently close to each other. Therefore, the effective performance of the proposed method in terms of the interaction between LTOs and RAF indices cannot be fairly studied. This is because the studied machine is not inherently eccentric due to manufacturing design, thus the LTOs amplitude is small. Therefore, the SWT of q -axis is not given in this section. Instead, studied test-rig is modified to properly realize the interaction between LTOs and RAF in the next subsection.

C. Emulation of LTOs by means of controlled brake units

In this subsection, a digital braking system with external torque excitation supplied is used to mimic the behavior of LTOs. To emulate the behavior of LTOs, torque reference signal is applied to the external control input of the control unit by means of a function generator. To study the behavior of LTOs in interaction with RAF indices, the frequency of torque oscillations is set at 8Hz as it can be observed in the spectrum of the external control input (Fig.9a). The rotational speed of WRIM with the regulation of external control input offset is set at 1365 rpm approximately. Therefore, the characteristic frequency of RAFs indices ($2sf_s$) will be 9 Hz. These two indices are as far apart as 1 Hz, which is significantly reduced from a value of about 16 Hz compared to the previous case (subsection B) (Fig.9b).

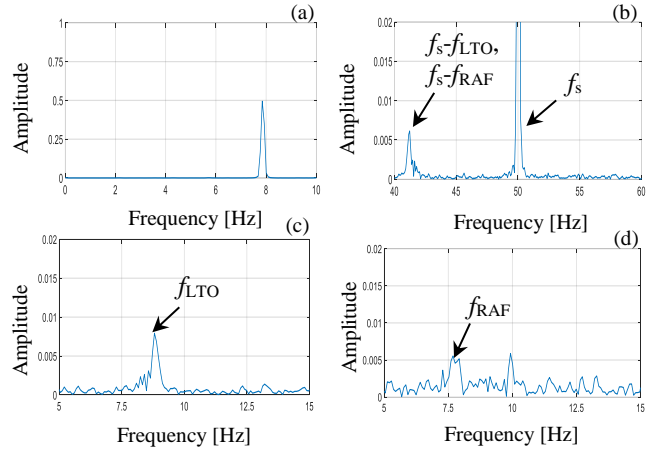


Fig.9. Experimental results in the case of the emulation of LTOs with controlled brake system in steady-state condition- a) Reference torque signal generated by function generator [0Hz-10Hz]- b) $i(f)$ - c) $i_d(f)$ - d) $i_q(f)$.

Although the index of RAF in the frequency of $(1 \pm 2s)f_s$ can be observed in the current spectrum, its overlap and proximity with LTOs, in times when there is no RAFs while LTOs exist, leads to false alarm (Fig.9b). From the proposed d -axis current spectrum, it is easy to detect the RAF index (9 Hz) while the LTOs index is eliminated (8 Hz) (Fig.9c). Furthermore, it is possible to detect the frequency of 8 Hz originated from LTOs in the q -axis current spectrum while no trace of RAFs index is visible (Fig.9d). The important point is that despite the coupling of rubber material, which leads to significant damping of LTOs, the effect of interaction between these two frequencies is well observed in the proposed d -axis of stator current. This indicates that in the case of rigid coupling, LTOs may be observed with greater clarity and magnitude on the motor shaft and thus in the proposed d -axis of stator current.

When the mass of the flywheel inertia is linked to the shaft as the load of the machine (subsection B), the magnitude of the LTO index is very small. Therefore, LTOs index cannot be well detected in the considerable distance from RAFs index. In fact, this is because the studied machine is not inherently eccentric due to manufacturing design. As a result, this index cannot be observed in the q -axis current. However, in this subsection, LTOs are applied to the machine by means of braking system and external excitation. Therefore, the magnitude of LTOs index, unlike the previous case, has a considerable amplitude and emerges near RAF index, which can be observed well in Fig.9c and Fig.9d.

The proposed method is also tested in the transient condition in which the braking system along with external control excitation is used (Fig.10). In order to test the proposed method and compare it with the simulation results, the currents of $\alpha\beta$ and dq axes and the variations of the machine speed are given in Fig.10. The test is carried out in deceleration mode where the speed of machine reduces from 1425 rpm to 1380 rpm (Fig.10a). The currents of $\alpha\beta$ are given in Fig.10b. It can be observed that the currents of $\alpha\beta$ axes are 90 degrees apart as it has been expected. Based of flowchart presented in Fig.2, the currents of d and q axes are given in Fig.10c and Fig.10d, respectively.

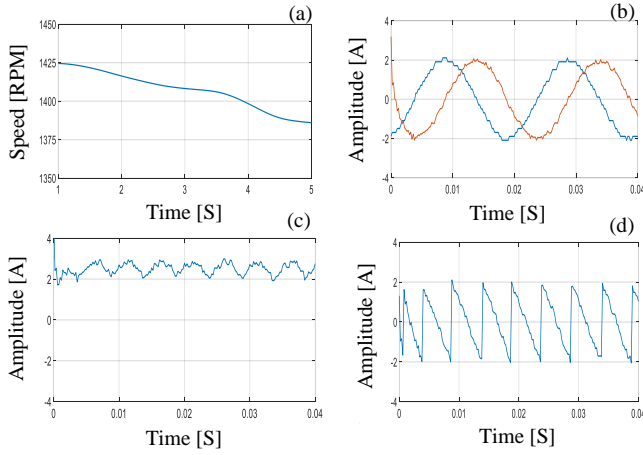


Fig.10. Experimental results in the case of the emulation of LTOs with controlled brake system in transient condition –a) Rotational speed of WRIG in deceleration condition –b) $i_a(t)$ and $i_b(t)$ –c) $i_d(t)$ –d) $i_q(t)$.

The current spectra of the d and q axes based on SWT technique well indicate the separation of the RAF index from the LTOs characteristic frequency, which are shown in Fig.11a. Since the braking system is used in torque control mode, the WRIG operates under speed variations originated from the oscillation in the torque of machine (Fig.11b). This can be well detected in the q -axis current spectrum (Fig.11b).

D. Comparison with previous methods

To compare and further explain the advantages of the proposed method, three relevant works are considered. For this purpose, fault detection methods using space harmonics, rectified stator current signature and square of the stator current of WRIM are compared (Fig.12). These methods are known for demodulation of RAF indices from supply frequency. Among them, the space harmonics of machines, which is considered as an alternative choice for rotor asymmetry fault detection (RAF) in the presence of LTOs, is given in Fig.12b.

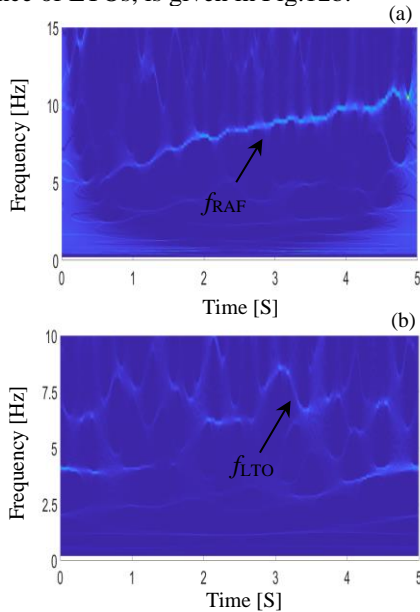


Fig.11. Time-frequency analysis of dq axes of stator current based on proposed technique in the case of the emulation of LTOs with controlled brake system in transient condition- a) SWT of $i_d(t)$ - b) SWT of $i_q(t)$.

It can be found that the fault characteristic frequencies cannot be clearly found in the spectrum of stator current due to inertia of machine and the level of noise similar to the spectrum of stator current signature without any pre-processing (Fig.12a). In this regard, the space harmonics of machine in the place of $(5-4s)f_s$ cannot be detected in the spectrum of stator current, properly (214Hz) [11]. Therefore, this method cannot be considered as a proper choice for isolation of RAF from LTOs. Recently, rectified stator current signature is used for demodulation of RAF from supply frequency [5]. Although this method can simply demodulate the RAF from the supply frequency, the isolation and separation of RAF from LTOs is not possible as it is shown in Fig.12c. In addition to these methods, the detection of fault based on square of stator current (I_s^2) is presented in Fig.12d in which the demodulation of LTOs and RAF from supply frequency is occurred. However, as seen, this method is unable to isolate RAF indices from LTOs [5].

It should be noted that the fundamental differences between the proposed method and some of the pervious methods are given in Table I. The number of sensors, the ability to demodulate fault indices from the supply frequency and transient analyses are the key factors for evaluation of the proposed methods as they have been stated in Table I. The proposed methods have priority in separation and isolation of fault indices from the supply frequency and LTOs based on these factors (Table I). Moreover, some of methods presented in Table I are invasive and needs installation of external sensors such as flux and mechanical rotor speed. The advantage of the proposed method in comparison with flux-based methods is its non-invasive nature of measuring the stator current.

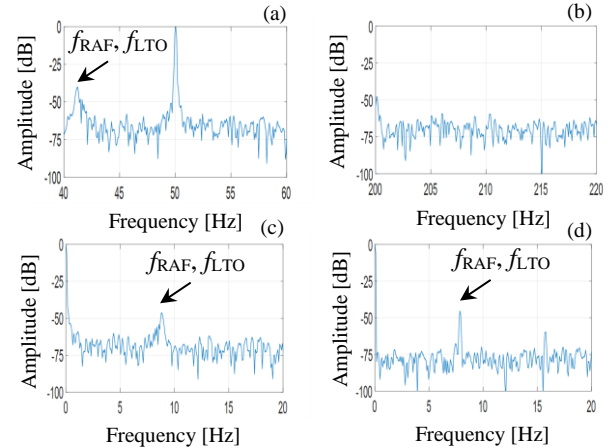


Fig.12. Comparison of proposed method with previous ones –a) Spectrum of stator current in the presence of LTOs in the vicinity of RAF indices –b) Detection and isolation of RAF in the Space harmonic of machine ($(5-4s)f_s$) –c) Spectrum of rectified stator current signature –d) Square of stator current spectrum

VI. CONCLUSION

In this paper, a new technique for separation of RAF characteristic frequencies from LTOs with single-phase of stator current is introduced. As solution, a new rotating reference frame is proposed. The method can effectively detect RAF indices from LTOs in the spectrum of d -axis of rotating reference frame even in line-fed induction machine. As results, the proposed method can be effectively used for isolation of

RAF from LTOs in order to avoid false alarm. Moreover, the method is validated in transient conditions through time-frequency analysis based on SWT technique. Since the method proposed in this manuscript is based on the use of single phase of machine, in order to remove RAF index from the q -axis current spectrum, the amplitudes of the fault characteristic frequency sidebands on both sides of the supply frequency need to be approximately equal to each other. However, when the braking system is used in speed control mode, in other words, LTOs are applied to the braking system in the form of speed oscillation; the amplitude of the left sideband is significantly larger than the right one. Therefore, LTOs cannot be detected in the q -axis of stator current.

REFERENCES

- [1] I. Zamudio-Ramirez, J. A. Antonino-Daviu, R. A. Osornio-Rios, R. de Jesus Romero-Troncoso and H. Razik, "Detection of Winding Asymmetries in Wound-Rotor Induction Motors via Transient Analysis of the External Magnetic Field," *IEEE Transactions on Industrial Electronics*, vol. 67, no. 6, pp. 5050-5059, June 2020.
- [2] M. H. Marzabali, S. H. Kia, H. Henao, G. Capolino and J. Faiz, "Planetary Gearbox Torsional Vibration Effects on Wound-Rotor Induction Generator Electrical Signatures," *IEEE Transactions on Industry Applications*, vol. 52, no. 6, pp. 4770-4780, Nov.-Dec. 2016.
- [3] M. H. Marzabali, J. Faiz, G. Capolino, S. H. Kia and H. Henao, "Planetary Gear Fault Detection Based on Mechanical Torque and Stator Current Signatures of a Wound Rotor Induction Generator," *IEEE Transactions on Energy Conversion*, vol. 33, no. 3, pp. 1072-1085, Sept. 2018.
- [4] H. Henao, G.-A. Capolino, M. Fernandez-Cabanias, F. Filippetti, C. Bruzzese, E. Strangas, R. Pusca, J. Estima, M. Riera-Guasp, and S. Hedayati-Kia, "Trends in Fault Diagnosis for Electrical Machines: A Review of Diagnostic Techniques," *IEEE Industrial Electronics Magazine*, vol. 8, no. 2, pp. 31-42, June 2014.
- [5] R. Puche-Panadero, J. Martinez-Roman, A. Sapena-Bano and J. Burriel-Valencia, "Diagnosis of Rotor Asymmetries Faults in Induction Machines Using the Rectified Stator Current," *IEEE Transactions on Energy Conversion*, vol. 35, no. 1, pp. 213-221, March 2020.
- [6] H. Li, G. Feng, D. Zhen, F. Gu and A. D. Ball, "A Normalized Frequency-Domain Energy Operator for Broken Rotor Bar Fault Diagnosis," *IEEE Transactions on Instrumentation and Measurement*, vol. 70, pp. 1-10, 2021, Art no. 3500110, doi: 10.1109/TIM.2020.3009011.
- [7] P. Balakrishna and U. Khan, "An Autonomous Electrical Signature Analysis-Based Method for Faults Monitoring in Industrial Motors," in *IEEE Transactions on Instrumentation and Measurement*, vol. 70, pp. 1-8, 2021.
- [8] V. Abolghasemi, M. H. Marzabali and S. Ferdowsi, "Recursive Singular Spectrum Analysis for Induction Machines Unbalanced Rotor Fault Diagnosis," in *IEEE Transactions on Instrumentation and Measurement*, vol. 71, pp. 1-11, 2022, Art no. 3500511, doi: 10.1109/TIM.2021.3129492.
- [9] M. Pineda-Sanchez, R. Puche-Panadero, M. Riera-Guasp, J. Perez-Cruz, J. Roger-Folch, J. Pons-Llinares, V. Clemente-Alarcon, J.A. Antonino-Daviu, "Application of the Teager-Kaiser Energy Operator to the Fault Diagnosis of Induction Motors," *IEEE Transactions on Energy Conversion*, vol. 28, no. 4, pp. 1036-1044, Dec. 2013.
- [10] F. B. Batista, P. C. M. Lamim Filho, R. Pederiva and V. A. D. Silva, "An Empirical Demodulation for Electrical Fault Detection in Induction Motors," *IEEE Transactions on Instrumentation and Measurement*, vol. 65, no. 3, pp. 559-569, March 2016.
- [11] H. Kim, S. B. Lee, S. Park, S. H. Kia and G. Capolino, "Reliable Detection of Rotor Faults Under the Influence of Low-Frequency Load Torque Oscillations for Applications With Speed Reduction Couplings," *IEEE Transactions on Industry Applications*, vol. 52, no. 2, pp. 1460-1468, March-April 2016.
- [12] O. Guellout, A. Rezig, S. Touati, and A. Djerdj, "Elimination of broken rotor bars false indications in induction machines," *Mathematics and Computers in Simulation*, p. In press, 2019. [Online]. Available: <http://www.sciencedirect.com/science/article/pii/S0378475419302083>.
- [13] R.R. Schoen, and T.G. Habetler, "Evaluation and implementation of a system to eliminate arbitrary load effects in current-based monitoring of induction machines," *IEEE Trans. on Ind. Appl.*, vol. 33, no. 6, pp.1571-1577, Nov./Dec. 1997.
- [14] C. Kral, H. Kapeller, F. Pirker, and G. Pascoli, "Discrimination of rotor faults and low frequency load torque modulations of squirrel cage induction machines by means of the Vienna monitoring method," *Proc. of PESC*, pp. 2861-2866, June 2005.
- [15] G. R. Bossio, C. H. De Angelo, J. M. Bossio, C. M. Pezzani, and G. O. Garcia, "Separating broken rotor bars and load oscillations on IM fault diagnosis through the instantaneous active and reactive currents," *IEEE Trans. Ind. Electron.*, vol. 56, no. 11, pp. 4571-4580, Nov. 2009.
- [16] J. Shin, Y. Park and S. B. Lee, "Flux-Based Detection and Classification of Induction Motor Eccentricity, Rotor Cage, and Load Defects," in *IEEE Transactions on Industry Applications*, vol. 57, no. 3, pp. 2471-2480, May-June 2021, doi: 10.1109/TIA.2021.3066960.
- [17] S. B. Lee, J. Shin, Y. Park, H. Kim and J. Kim, "Reliable Flux-Based Detection of Induction Motor Rotor Faults From the Fifth Rotor Rotational Frequency Sideband," in *IEEE Transactions on Industrial Electronics*, vol. 68, no. 9, pp. 7874-7883, Sept. 2021, doi: 10.1109/TIE.2020.3016241.
- [18] Dias, Cleber Gustavo, Luiz Carlos Da Silva, and Ivan Eduardo Chabu. "Fuzzy-based statistical feature extraction for detecting broken rotor bars in line-fed and inverter-fed induction motors." *Energies* 12.12 (2019): 2381.
- [19] Dias, Cleber Gustavo, Luiz Carlos da Silva, and Wonder Alexandre Luz Alves. "A histogram of oriented gradients approach for detecting broken bars in squirrel-cage induction motors." *IEEE Transactions on Instrumentation and Measurement* 69.9 (2020): 6968-6981.
- [20] M. Drif, H. Kim, J. Kim, S. B. Lee and A. J. M. Cardoso, "Active and Reactive Power Spectra-Based Detection and Separation of Rotor Faults and Low-Frequency Load Torque Oscillations," *IEEE Transactions on Industry Applications*, vol. 53, no. 3, pp. 2702-2710, May-June 2017.
- [21] S. H. Kia, H. Henao and G. Capolino, "Analytical and Experimental Study of Gearbox Mechanical Effect on the Induction Machine Stator Current Signature," *IEEE Transactions on Industry Applications*, vol. 45, no. 4, pp. 1405-1415, July-Aug. 2009.
- [22] J. Zhang, J. Hang, S. Ding and M. Cheng, "Online Diagnosis and Localization of High-Resistance Connection in PMSM With Improved Fault Indicator," *IEEE Transactions on Power Electronics*, vol. 32, no. 5, pp. 3585-3594, May 2017.
- [23] J. Yun, J. Cho, S. B. Lee and J. Yoo, "Online Detection of High-Resistance Connections in the Incoming Electrical Circuit for Induction Motors," *IEEE Transactions on Industry Applications*, vol. 45, no. 2, pp. 694-702, March-april 2009.
- [24] M. Mengoni, L. Zarri, Y. Gritli, A. Tani, F. Filippetti and S. B. Lee, "Online Detection of High-Resistance Connections With Negative-Sequence Regulators in Three-Phase Induction Motor Drives," *IEEE Transactions on Industry Applications*, vol. 51, no. 2, pp. 1579-1586, March-April 2015.
- [25] M. Feldman, *Hilbert Transform Applications in Mechanical Vibration*. Hoboken, NJ, USA: Wiley, 2011.
- [26] X. Tu, Y. Hu, F. Li, S. Abbas, Z. Liu and W. Bao, "Demodulated High-Order Synchro-squeezing Transform With Application to Machine Fault Diagnosis," in *IEEE Transactions on Industrial Electronics*, vol. 66, no. 4, pp. 3071-3081, April 2019, doi: 10.1109/TIE.2018.2847640.
- [27] Liu, Qi, Yanxue Wang, and Yonggang Xu. "Synchrosqueezing extracting transform and its application in bearing fault diagnosis under non-stationary conditions." *Measurement* 173 (2021): 108569.
- [28] Liu, Wei, Wei Chen, and Zhihua Zhang. "A novel fault diagnosis approach for rolling bearing based on high-order synchrosqueezing transform and detrended fluctuation analysis." *IEEE Access* 8 (2020): 12533-12541.
- [29] J. Shin, Y. Park and S. B. Lee, "Flux-Based Detection and Classification of Induction Motor Eccentricity, Rotor Cage, and Load Defects," in *IEEE Transactions on Industry Applications*, vol. 57, no. 3, pp. 2471-2480, May-June 2021, doi: 10.1109/TIA.2021.3066960.
- [30] Garcia-Calva, Tomas A., Daniel Morinigo-Sotelo, Vanessa Fernandez-Cavero, Arturo Garcia-Perez, and Rene de J. Romero-Troncoso. "Early detection of broken rotor bars in inverter-fed induction motors using speed analysis of startup transients." *Energies* 14, no. 5 (2021): 1469.
- [31] Park, Yonghyun, et al. "Airgap flux based detection and classification of induction motor rotor and load defects during the starting transient." *IEEE Transactions on Industrial Electronics* 67.12 (2020): 10075-10084.
- [32] Garcia-Calva, Tomas Alberto, Daniel Morinigo-Sotelo, and Rene De Jesus Romero-Troncoso. "Fundamental Frequency Normalization for Reliable Detection of Rotor and Load Defects in VSD-fed Induction Motors." *IEEE Transactions on Energy Conversion* (2021).